10-23-2017

N (2P) production in electron-N2 collisions

Wladyslaw Kedzierski
University of Windsor

Jeff Dech
University of Windsor

J. W. Mcconkey
University of Windsor

N (^{2}P) Production in electron-N_2 Collisions.

W Kedzierski, J Dech and J W McConkey

Physics Department, University of Windsor, ON N9B 3P4, Canada.

Abstract:

A unique detector which is selectively sensitive to low energy metastable atoms, has been used to study the production of ground state N (^{2}P) atoms following collisions of low energy (0-200 eV) electrons with molecular nitrogen. TOF techniques have revealed the existence of at least two distinct mechanisms yielding this dissociation product. Released kinetic energies in the dissociation have allowed positioning of the parent molecular states in the Franck-Condon region. This has allowed probable parent states, such as B' $^3\Sigma_u^-$, b' $^1\Sigma_u^+$ and C' $^3\Pi_u$, to be identified making use of recent theoretical calculations. Both direct and pre-dissociation processes are shown to be involved.

Introduction:

Ever since the first observation [1] in the laboratory of so-called “forbidden” radiation between the states of the ground configuration of atomic nitrogen, these metastable atoms have been found to play a significant role in many fields ranging from active nitrogen flowing afterglows [2] to the aurora [3]. Because of their excitation energy the metastables are highly reactive playing an important role in the chemistry of Earth’s upper atmosphere [4], in the atmospheres of other planets and moons in the solar system [5,6] as well as in combustion [7], discharge chemistry and plasma processing [8]. They have been used recently in Zeeman slowing experiments [9]

For convenience the ground configuration of atomic nitrogen, together with the main transitions which occur, is shown in Figure 1. In the present work we shall be

dealing with the $^2P_{1/2, 3/2}$ state which has a lifetime of more than a second and decays to lower levels via magnetic dipole transitions at 1040 and 346.6 nm.

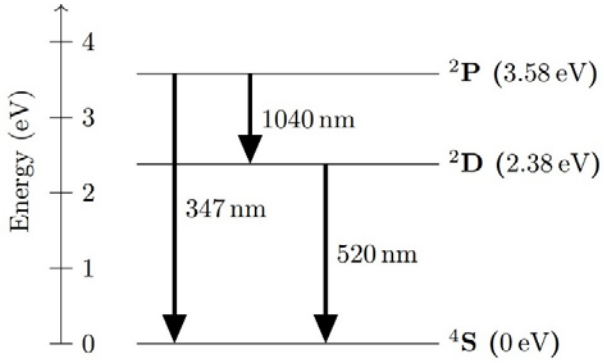

Figure 1. Energy levels within the ground configuration of atomic N and transitions between them.

Some earlier research which is relevant to the present work is the 1924 work of Vegard [10] and McLennan and Shrum [11], who bombarded solid N_2 with electrons and "canal rays" and observed the resultant fluorescence, and the work of Broida's group some three decades later [12] where the products of a flowing discharge in N_2 were condensed on a surface at 4.2 K and again emitted a long-lived fluorescence near 523 nm. This emission was identified as due to the atomic ^{2}D - ^{4}S transitions which in the gas phase occur at a slightly lower wavelength (Figure 1). Herzfeld and Broida [12] also observed a weaker line emission at 346.96 nm which they associated with the ^{2}P - ^{4}S transitions which have a gas phase wavelength of 346.65 nm [13]. In previous work involving detection of the equivalent low-lying metastable states of atomic oxygen [14] we were able to use spectral information from experiments [15] where fluorescence was observed from small amounts of oxygen frozen in rare gas matrices when bombarded with high energy electrons. The wavelengths of this fluorescence acted as a guide to where in the spectrum we might expect radiation using the novel solid-rare-gas detector which we employ also in this work.

Apparatus.

The equipment which we used in this work has been described extensively elsewhere [15] so only a brief summary will be included here. A crossed electron-N_2 beam system is used with detection of dissociation products in a separate chamber located orthogonally to the two beams. Background pressure in the vacuum system was 10^{-7} torr. This rose to approximately 10^{-5} torr when the gas beam was introduced. The e-beam is pulsed (27 μs width) and the resultant

metastables drift to a solid xenon surface held at 18K Here they form excimers which immediately radiate. The resultant photons are detected using a photomultiplier-filter combination. Time-of-flight (TOF) techniques are used to separate these photons from prompt photons produced in the initial electron-N_2 collision. The excimer emission is observed using a 10 nm bandpass filter centered on 340 nm. This filter also transmits the N_2 $C^3\Pi_u - B^3\Pi_g$ (0,0) 337 nm Second Positive band which was used for energy calibration as discussed later. Use of this filter was found to be essential as a large background arising from stray scattered light from the filament of the e-beam source would otherwise swamp the emission. This background increased in magnitude towards the red end of the spectrum and was possibly one reason why we were unable to observe any signal near 520 nm which was where radiation from the ^2D metastable state was expected. Quench plates in the path of the metastables to the detector allow a check for any high-Rydberg species which might be present. No such species were detected in the present experiment.

Results and Discussion.

Figure 2 shows a TOF spectrum taken at an impact energy of 100 eV. In addition to the prompt photon peak at very short times coincident with the e-beam pulse we note the presence of two structures at longer times corresponding to the arrival of two groups of metastable atoms. As indicated on Figure 2, it was possible to separate the two components using Gaussian functions. As discussed later, these were used to obtain information about the released kinetic energy distributions represented by these two channels. The peaks correspond to total released kinetic energies of 2.7 and 0.56 eV. The slower group has contributions from atoms arriving up to about 300 μs after the current pulse. This corresponds to a total released kinetic energy of about 0.1 eV i.e. the parent dissociating state must have a threshold energy very close to the dissociation threshold for production of $N(^2P)$. This is confirmed by threshold measurements discussed below.

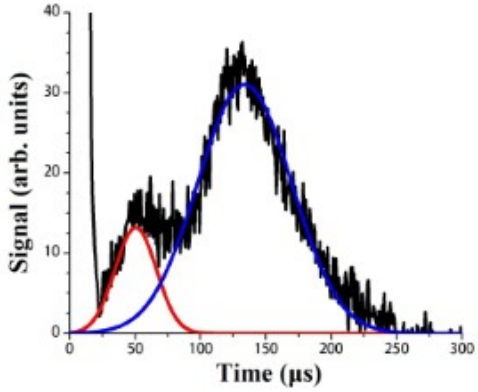

Figure 2. TOF spectrum taken at an impact energy of 100eV. The truncated peak at very short times is due to prompt photons emitted in coincidence with the exciting electron beam pulse. The metastable data can be represented by the sum of the two Gaussian functions shown.

By isolating data for atoms arriving between 100 and 200 μs and studying production of these atoms as a function of exciting electron energy, we obtain the graph shown in Figure 3. This graph also shows the excitation probability curve for the prompt photons (the (0,0) C $^3\Pi_u \rightarrow$B $^3\Pi_g$ Second Positive band at 337.1 nm) The peak in this band at 14 eV [16, 17] allows the energy axis to be calibrated.

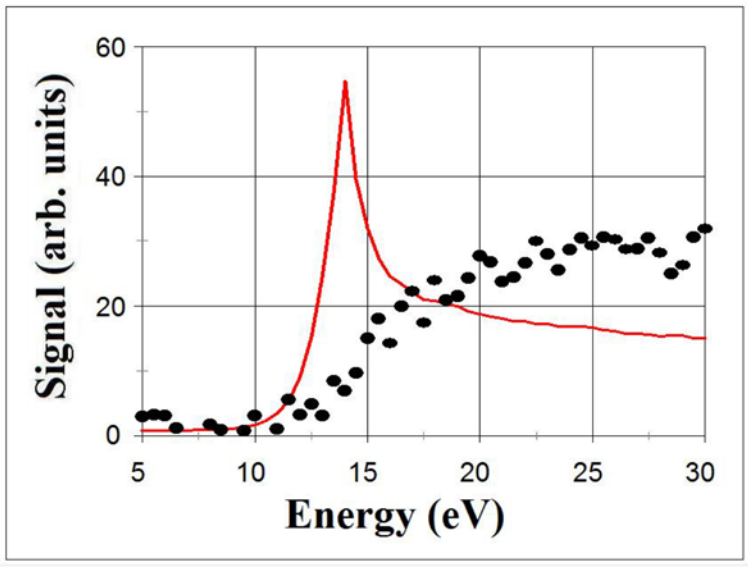

Figure 3. Excitation probability curves for the C $^3\Pi_u \rightarrow$ B $^3\Pi_g$ (0,0) Second Positive band (sharp peak at 14 eV) and the metastables arriving in the TOF window between 100 and 200 μs. See text for further details. A large background has been subtracted from the metastable signal.

Although the statistical quality of the metastable signal is poor it is clear that the threshold for production of N (^{2}P) is close to 13 eV. Since the minimum energy for production of N (^{2}P) with a ground state N (^{4}S) partner is 13.33 eV, it is evident that the direct dissociative process

$$e + N_2 (X\ ^1\Sigma_g^+, v = 0) \rightarrow e' + N_2^* \rightarrow N\ (^2P) + N\ (^4S) \qquad (1)$$

is a strong contributor to the metastable signal with the initial excitation being to the inner wall of the parent potential energy curve. This is illustrated in Figure 4 drawn from the work of Hochlaf et al [24] which shows the various curves which are based on the N(^{2}P) + N(^{4}S) limit. The Franck-Condon region is also shown on Figure 4 to highlight the possible excitation routes. Clearly the B' $^3\Sigma_u^-$ state is a likely candidate for N_2* in Equation 1.

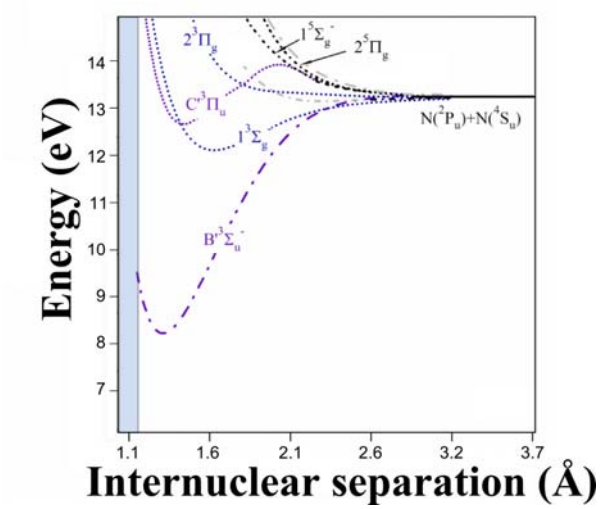

Figure 4. Potential energy curves for states which are based on the N(^{2}P) + N(^{4}S) dissociation limit. Data are taken from the calculations of Hochlaf et al [24]. The Franck-Condon region governing excitation from the N_2 $^1\Sigma_g^+$, v=0 ground state is shown shaded.

Pre-dissociation of one or more of the states at higher excitation energy is probably also contributing. Cosby [27] studied the dissociation of N_2 into neutral ground state fragments and found strong evidence for pre-dissociation mainly into N(^{4}S) and N(^{2}D) but also weakly into N(^{2}P). Ajello et al [28] in their detailed study of

electron impact excitation of the c_4' and b' $^1\Sigma_u^+$ states demonstrated significant occurrence of pre-dissociation particularly in the latter case where they estimated that 84% of the excitation led to pre-dissociation. Many of the vibrational levels of the b' $^1\Sigma_u^+$ state lie at energies above the N (^{2}P) + N (^{4}S) limit. Assuming the b' $^1\Sigma_u^+$ state is responsible, the process may be represented by Equation 2 and is illustrated in Figure 5 using the calculated curves taken from the work of Little and Tennyson [25].

$$e + N_2 (X\ ^1\Sigma_g^+, v = 0) \rightarrow e' + N_2 (b'\ ^1\Sigma_u^+, v) \rightarrow N_2^*(\text{pre-diss}) \rightarrow N(^2P) + N(^4S) \quad (2).$$

Some singlet-triplet mixing must also be involved since only states of triplet and higher multiplicities lead to production of the atom states represented by Equation 2.

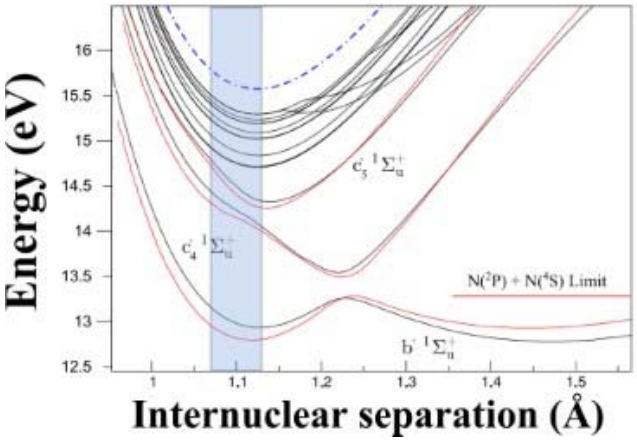

Figure 5. High-lying potential energy curves for the Rydberg states of $^1\Sigma_u^+$ symmetry. Data taken from the calculations of Little and Tennyson [25].The Franck-Condon region governing excitation from the N_2 ($^1\Sigma_g^+$, v=0) ground state is shown shaded and the N (^{2}P) + N (^{4}S) limit is indicated. The dashed line indicates the ground state of N_2^+. The duplicate nature of some of the curves reflects a comparison between the calculations of References 25 and 26.

Figure 6 presents the metastable excitation probability data over a wider energy range up to 180 eV. Even though the statistical quality of the data is poor, there appears to be a rapid rise from threshold to a shoulder around 25-30 eV followed by an increase to a broad maximum around 75 eV and a slow fall off to higher energies.

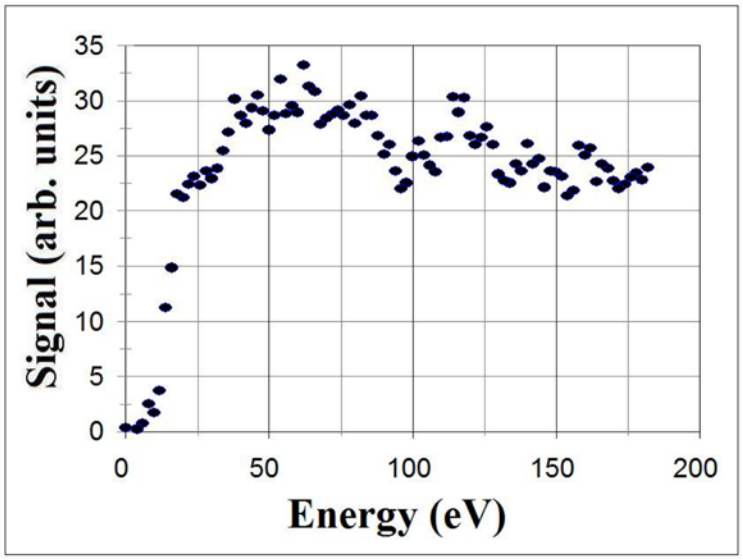

Figure 6. Slow metastable excitation probability curve from threshold to 180 eV. Experimental parameters are similar to those in Figure 3 except higher e-beam currents were used to help gain better statistical quality. Some smoothing has been applied to the data.

This overall shape would support the two channel excitation model, such as suggested by Equations 1 and 2, with one channel involving a spin flip dominating the near threshold region and a second channel yielding a rather broad excitation function to higher energies consistent with a process where no change of multiplicity in the initial excitation occurred.

Because of the weak signal strengths it was not possible to obtain separate excitation probability data for the faster metastable component – peaked around 50 μs TOF, Figure 1. To gain some additional information we have carried out a transformation from TOF to corresponding released kinetic energy. The total released kinetic energy spectrum which best fits the data of Figure 2 is shown in Figure 7. Because of the rather poor statistical quality of the TOF data, the TOF curve was fitted first with the sum of two Gaussian functions and then a TOF to energy transformation was carried out for the complete TOF curve and for each Gaussian separately using the procedure given by Smyth et al [20]. The total kinetic energy released was shared equally between the two N-fragments. The two peaks evident on the TOF data transform into a lower energy peak with released kinetic energies ranging up to about 2 eV and a very broad, higher energy structure peaking around 3 eV but extending from 1 to about 7 eV.

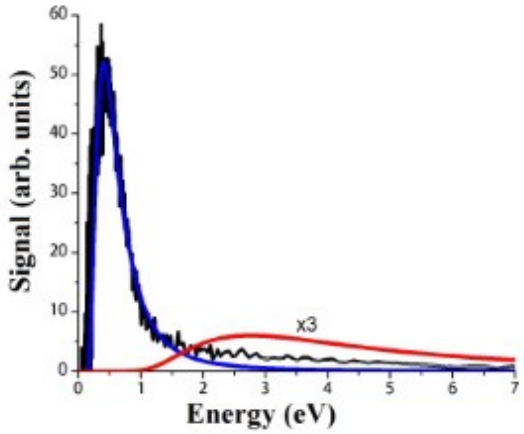

Figure 7. Plot of total released kinetic energy in the N_2 dissociation. The picture is obtained from the TOF data of Figure 2 using the procedure discussed in the text. The solid lines represent the contributions from the Gaussian TOF distributions of Figure 2. Note that the higher energy data group has been multiplied by 3 to demonstrate its shape more clearly.

The released kinetic energy range of the faster metastable data means that the parent excited state potential energy curve must cross the Franck- Condon region steeply in the 14-19 eV region if the same dissociation limit as in Equations 1 and 2 is assumed. Individual TOF data sets taken with impact energies as low as 30 eV clearly showed both peaks. However, the relative heights of the two metastable peaks taken at low (35 eV) and high (300 eV) energies indicated that the excitation probability curve for the higher energy group was less sharply peaked at lower energies, suggesting that near-threshold spin-flip excitation in the parent molecule was not as dominant in this instance.

Of the numerous calculations of the high lying states of N_2 [e.g. 21-26] we show in Figure 4, taken from Ref 24, some possible excitation channels which might be open in the present instance. For example the repulsive inner potentials of the C' $^3\Pi_u$ and 1 $^3\Sigma_g$ states are seen to cross the Franck-Condon region at energies greater than 15 eV. Thus excitation to these states would yield total dissociation energies greater than about 1.7 eV in reasonable agreement with our estimates, Figure 7. We note that whatever state or states are involved they must also display some singlet admixture so that excitation to higher electron impact energies remains relatively strong.

We note finally that excitation of N (^{2}P), via higher-lying parent states dissociating to higher energy limits involving a partner other than N (^{4}S), is unlikely to be significant since such states would probably produce higher energy fragment kinetic energies than were observed here.

Conclusions.

Dissociative excitation of N_2 has been studied using a novel detector which is selectively sensitive to N (^{2}P) metastable atoms. TOF techniques have revealed the existence of two distinct excitation channels, or groups of excitation channels, yielding this dissociation product. Released kinetic energies in the dissociation have allowed positioning of the parent molecular states in the Franck-Condon region. This has allowed probable parent states to be identified making use of recent theoretical calculations. Both direct and pre-dissociation processes are shown to be involved

Acknowledgements.
The authors gratefully acknowledge financial support from NSERC (Canada) and CFI (Canada) and invaluable technical support from the University of Windsor, Physics Department, mechanical and electronic workshops.

References:

1. Kaplan J, Phys Rev, **55**, 598 and 858, (1939).

2. Lin C and Kaufman F, J Chem Phys, **55**, 3760, (1971).

3. Zipf E C, Espy P J and Boyle C F, J Geophys Res, Space Phys, **85**, 687, (1980).

4. Chakrabarti S, J Atmos Sol-Terr Phys, **16**, 1403, (1998)

5. Bakalian F, Icarus, **183**, 69, (2006).

6. Imanaka H and Smith M A, Proc Natl Acad Sci, USA, **107**, 12423, (2010).

7. Baulch D L et al, J Phys Chem Ref Data, **34**, 757, (2005).

8. Heron J T, J Phys Chem Ref Data, **2**8, 1453, (1999).

9. Dulitz K, Toscano J, Tauschinsky A and Softley T P, J Phys B, **49**, 075203, (2016).

10. Vegard L, Nature, **113**, 716, (1924).

11. McLennan J C, and Shrum G M, Proc Roy Soc (London), **A106**, 138, (1924).

12. Herzfeld C M and Broida H P, Phys Rev, 101, 606, (1956).

13. McConkey J W and Herman L, Phys Lett, **12**, 13, (1964).

14. McConkey J W and Kedzierski W, Adv At Mol Opt Phys, **63**, 1, (2014).

15. Schoen L J and Broida H P, J. Chem. Phys. **32**, 1184–1193, (1960).
16. Burns D J, Simpson F R and McConkey J W, J Phys B, **2**, 52, (1969).
17. Shemansky D E, Ajello J M and Kanik I, Astrophys J, **452**, 472, (1995) and included references.
18. Tilford S G and Wilkinson P G., Am. J. Mol. Spectrosc. **12**, 231, (1964).
19. Lofthus A and Krupenie P H, J Phys Chem Ref Data, **6**, 113, (1977).
20. Smyth, K.C., Schiavone, J.A. and. Freund R.S., J. Chem. Phys. **59**, 5225, (1973).
21. H. H. Michels, in Electronic structure of excited states of selected atmospheric systems", Ed. J. W. McGowan, Advanced Chemical Physics **45**, 225 (1981).

22. W. C. Ermler, A. D. McLean and R. S. Mulliken. J. Phys. Chem. **86**, 1305, (1982).
23. W C Ermler, J P Clark and R S Mulliken, J Chem Phys, 86, 370, (1987).
24. M Hochlaf, H Ndome, D Hammoutene and M Vervloet, J Phys B, **43**, 245101, (2010).
25. D A Little and J Tennyson, J Phys B, **46**, 145102, (2013).
26. D Spelsberg and W Mayer, J Chem Phys, 115, 6435, (2001).
27. P C Cosby, J Chem Phys, **98**, 9544, (1993).
28. J M Ajello, G K James, B O Franklin and D E Shemansky, Phys Rev A, **40**, 3524, (1989).